

Dual-Band, Low-Frequency Artificial Magnetic Conductor using Lumped Components

G. Lasser,¹ Z. Popović² and C. F. Mecklenbräuer¹

¹Vienna University of Technology, Gusshausstraße 25/389, Austria
Christian Doppler Laboratory for Wireless Technologies for Sustainable Mobility

²Univ. of Colorado, Boulder, USA
gregor.lasser@nt.tuwien.ac.at

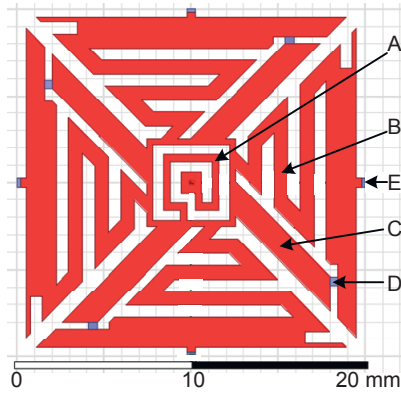
Abstract – In this contribution we discuss the design of a Frequency Selective Surface (FSS) serving as planar, dual-band, low-frequency Artificial Magnetic Conductor (AMC). The unit cell geometry of the AMC is based on meander structures to reduce its size and allow for the design of two separately tuneable resonances. The FSS is constructed from two single-sided Printed Circuit Boards (PCBs) manufactured from cost-effective FR-4 separated by nylon spacers. The unit cells contain lumped elements for tuning of the individual resonances and immunity to permittivity variations of the substrate. The numerical simulation results are discussed and compared to measurements obtained from manufactured specimens.

I. INTRODUCTION

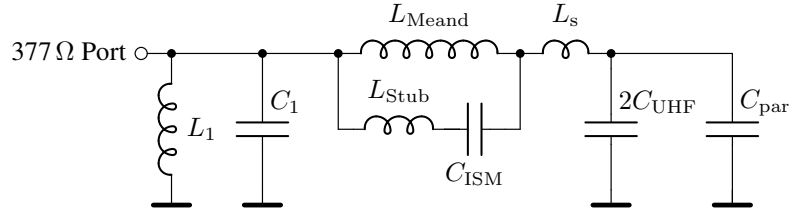
In the recent years the beneficial use of AMCs for antenna applications has gained much interest [1, 2]. In this contribution we describe and characterize a cost-effective, dual-band FSS that resembles an AMC which operates at 868 MHz and 2.45 GHz and is intended to improve the performance of a switched-beam antenna [3]. While [4] reports on the antenna performance of the overall antenna system including the AMC this contribution focuses on the implementation and characterization of the manufactured AMC panels, which uses lumped elements to overcome the permittivity production tolerances of cost effective Printed Circuit Board (PCB) substrates.

II. IMPLEMENTATION

Since the FSS is designed for operation in the near field of an antenna, the unit-cell dimensions should be small when compared to the wavelengths. The classical Sievenpiper mushroom unit cells are relatively big and so an AMC constructed from such cells often cannot be considered as a homogeneous surface. The unit cell dimensions depend on the substrate height and patch spacing — decreasing both parameters reduces the unit cell size while keeping the resonance frequency constant. But this method also reduces the AMC bandwidth and increases the sensitivity of the resonance frequency to manufacturing tolerances. In this contribution we present an AMC constructed of two single-sided PCBs spaced by nylon spacers. Both PCBs have their copper layers facing outwards. The bottom PCB serves as ground plane, while the metallization of the top PCB is structured to form the unit cells. The PCBs with dimensions 300 mm × 300 mm × 1.5 mm are spaced 8 mm and are interconnected using tinned copper wire with 0.51 mm diameter. Our AMC uses lumped components as presented in [5]. The unit cell geometry is shown in Fig. 1a. We use meander structures similar to [6, 7] to reduce the size of the unit cell and create two separately tuneable resonances. Each unit cell is composed of four identical quadrants which are connected in the centre and further connected to the centre inductor (Fig. 1aA) which finally leads to a via to the groundplane. This inductor does not alter the AMC resonance frequencies but lowers the Transversal Magnetic (TM) plasmon frequency. The meander line (Fig. 1aB) and the inter-cell capacitor $C_{\text{UHF}} = 0.4$ pF (E) set the first resonance frequency at 868 MHz. The second resonance at 2.45 GHz is created by bypassing the meander line with a direct stub (C) and a series capacitor $C_{\text{ISM}} = 0.2$ pF (D) which is chosen small enough not to disable the meander inductance for low frequencies. The described geometry allows for a unit cell size in terms of the free space wavelengths of $0.058 \lambda_0$ at 868 MHz and $0.163 \lambda_0$ at 2.45 GHz.



(a) Geometry of the unit cell. The copper is plotted in red, the blue areas indicate lumped capacitor positions.



(b) Equivalent circuit model for the developed AMC structures.

Fig. 1: Unit cell geometry and equivalent circuit.

III. EQUIVALENT CIRCUIT MODEL

The design of the FSS structure was aided by Finite Element Method (FEM) simulations which are time consuming. To speed up the simulation process we developed the equivalent circuit model shown in Fig. 1b. This model is used to predict the phase response for a plane wave and normal incident in the interesting frequency range from Direct Current (DC) to approximately 4 GHz very accurately. Most model elements are directly related to physical features of the FSS geometry, so new FEM simulations are now started with suitable values for fine tuning. The capacitors $2C_{\text{UHF}}$ and C_{ISM} directly relate to the discrete capacitors in the FSS. The shunt capacitor to ground $2C_{\text{UHF}}$ is twice the value of the inter-element capacitor used to tune the Ultra High Frequency (UHF) frequency, since it is connected to ground and not to the next cell. The inductances on the right also directly refer to physical properties: The inductance of the shortening stub for 2.45 GHz is L_{Stub} , the meander Inductance L_{Meand} , and L_s corresponds to the small series inductance of the last patch which connects the meander to the edge capacitor, and the inductance of the centre square surrounding the centre inductor. The parasitic capacitance between the neighbouring unit cells is modelled with C_{par} . The tank circuit $L_1 C_1$ corresponds to the interaction between the top layer of the FSS and the bottom ground-plane. The circuit is excited using a port with a source impedance of 377Ω corresponding to the free space wave impedance. All component values for the model except $2C_{\text{UHF}}$ and C_{ISM} were found by curve fitting the phase response curves for various simulated phase responses for different capacitor values and are found in Table 1. The model is most helpful to evaluate which meander lengths and capacitor values lead to which bandwidths of the corresponding resonance frequencies.

Table 1: Values of equivalent circuit model for FSS1.

	L_1	C_1	L_{Meand}	L_{Stub}	L_s	C_{par}	$2C_{\text{UHF}}$	C_{ISM}
Value in pF / nH	10.55	0.48	9.00	6.73	3.00	0.75	0.80	0.20

IV. MEASUREMENT RESULTS

The phase response of the AMC panels for a plane normal incident wave were measured in an anechoic chamber using a measurement setup similar to the one described in [1, Fig. 13] using two ridged horn antennas placed side by side connected to a network analyser. The measurements agreed very well to the simulations, despite the use of RF-4 substrate. The relative bandwidths of the resonance frequencies are 10 % at 868 MHz and 20 % at 2.45 GHz.

To analyse the stop-band behaviour regarding surface waves the eigenmodes of an infinite FSS constructed from the proposed unit cells are simulated, see the band structure diagram in Fig. 2a. We note that the dashed lines corresponding to our AMC resonance frequencies are laying in stop bands of the FSS. We measured the surface wave transmission gain when compared to a copper plate of identical size as the FSS panel using the method

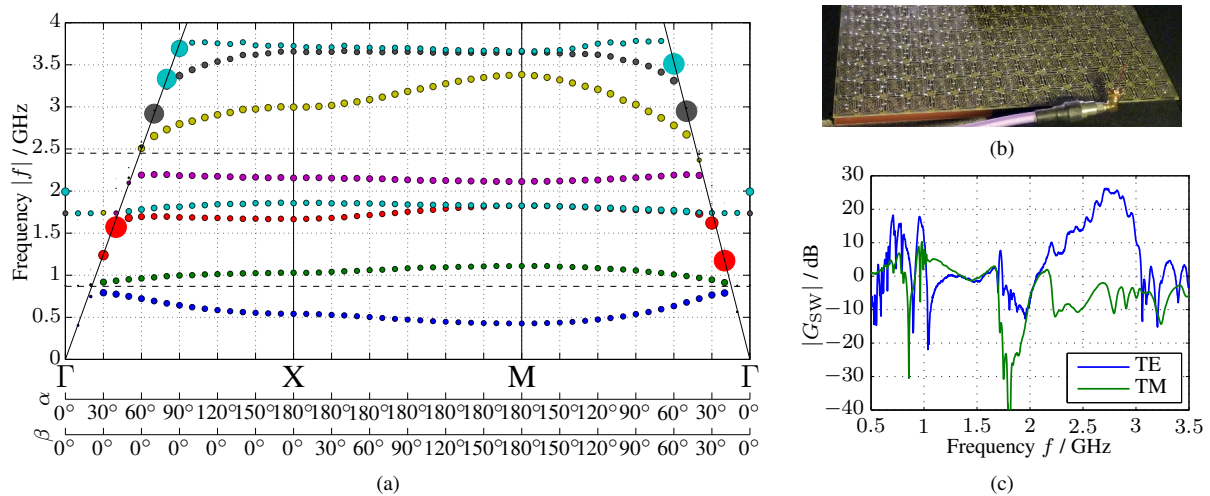


Fig. 2: Surface wave analysis:(a) Simulated band structure diagram. Different colours indicate different modes. The marker size is proportional to the Q of the corresponding mode. The slanted black lines correspond to the free space light lines. (b) Photograph of TM surface waves measurement setup. (c) Measured surface wave gain G_{SW} of the AMC panel when compared to a GP of the same size.

[1, Fig.11], the results are shown in Fig. 2c. While the measured low-frequency stop band is quite narrow, the 2.45 GHz stop band for TM waves is spread but not very distinct. For Transversal Electric (TE) modes we do not see a stop band in our measurement results — probably due to the small AMC panel size.

V. CONCLUSION

In this contribution we present and characterize a dual-band AMC constructed from two PCBs manufactured from low-cost FR-4 separated by nylon spacers. The unit cells contain meander structures and lumped capacitors to shrink the size of the cells to $0.058 \lambda_0$ at 868 MHz and $0.163 \lambda_0$ at 2.45 GHz. We present an equivalent circuit model very helpful to quickly find a tradeoff between the AMC resonance bandwidth, which were measured to be 10% and 20% at the low and high band. An eigenmode analysis shows stop bands at the desired frequencies which could be verified for TM modes in measurements.

ACKNOWLEDGEMENT

This work has been funded by the Christian Doppler Laboratory for Wireless Technologies for Sustainable Mobility.

REFERENCES

- [1] D. Sievenpiper, L. Zhang, R. F. Jimenez Broas, N. G. Alexopolous, and E. Yablonovitch, "High-impedance electromagnetic surfaces with a forbidden frequency band," *IEEE Trans. Microw. Theory Tech.*, vol. 47, no. 11, pp. 2059–2074, Nov. 1999.
- [2] A. P. Feresidis, G. Goussetis, S. Wang, and J. Y. C. Vardaxoglou, "Artificial magnetic conductor surfaces and their application to low-profile high-gain planar antennas," *IEEE Trans. Antennas Propag.*, vol. 53, no. 1, pp. 209–215, Jan. 2005.
- [3] G. Lasser, L. W. Mayer, and C. F. Mecklenbräuker, "Compact low profile UHF switched-beam antenna for advanced tyre monitoring systems," in *2012 IEEE-APS Topical Conference on Antennas and Propagation in Wireless Communications*, Kapstadt, Sep. 2012.
- [4] G. Lasser, L. W. Mayer, Z. Popović, and C. F. Mecklenbräuker, "Low-profile switched-beam antenna backed by an artificial magnetic conductor for efficient close to metal operation," 2015, submitted to *IEEE Trans. Antennas Propag.*
- [5] M. Bray and D. Werner, "A novel design approach for an independently tunable dual-band EBG AMC surface," in *Antennas and Propagation Society International Symposium, 2004. IEEE*, vol. 1, Jun. 2004, pp. 289–292 Vol.1.
- [6] M. F. Abedin, M. Z. Azad, and M. Ali, "Wideband smaller unit-cell planar ebg structures and their application," *IEEE Trans. Antennas Propag.*, vol. 56, no. 3, pp. 903–908, Mar. 2008.
- [7] D. J. Kern, D. H. Werner, A. Monorchio, L. Lanuzza, and M. J. Wilhelm, "The design synthesis of multiband artificial magnetic conductors using high impedance frequency selective surfaces," *IEEE Trans. Antennas Propag.*, vol. 53, no. 1, pp. 8–17, Jan. 2005.